Electronic supplementary information (ESI)

Mechanism of the generation of ultra-stable radicals in fast photochromic naphthalenediimide-based coordination polymers

Shimin Zhang[a,b], Pengfei Hao[b], Yifang Zhang[b], Gaopeng Li[b], Junju Shen[b], Haiying Yang[a] and Yunlong Fu*[b]*

a. Department of Applied Chemistry, Yuncheng University, Yuncheng 044000, China

b. Key Laboratory of Magnetic Molecules & Magnetic Information Materials Ministry of Education, School of Chemical and Material Science, Shanxi Normal University, Taiyuan 030031, China

Contents

1. Figure

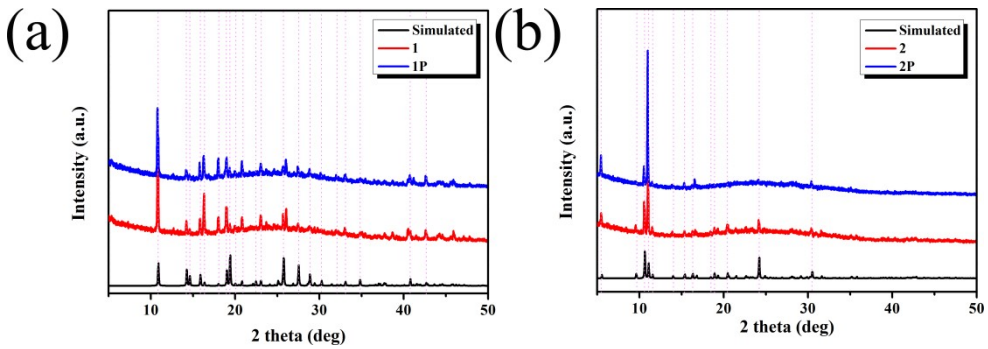

Fig. S1. (a) PXRD patterns of **1** and **1P** at room temperature. (b) PXRD patterns of **2** and **2P** at room temperature.

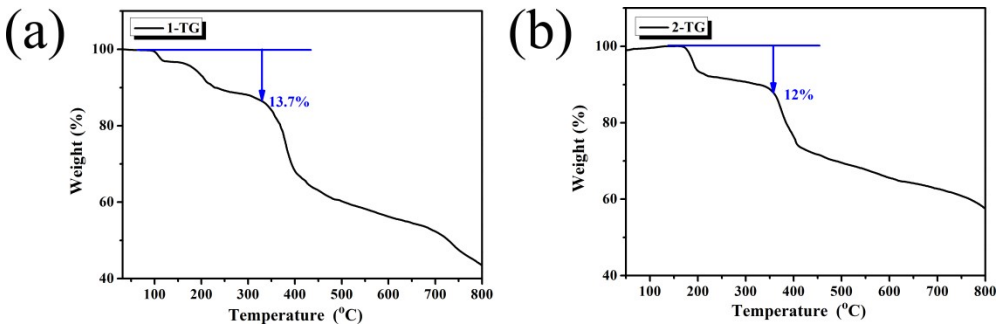

Fig. S2. (a) TGA curve of **1**. (b) TGA curve of **2**.

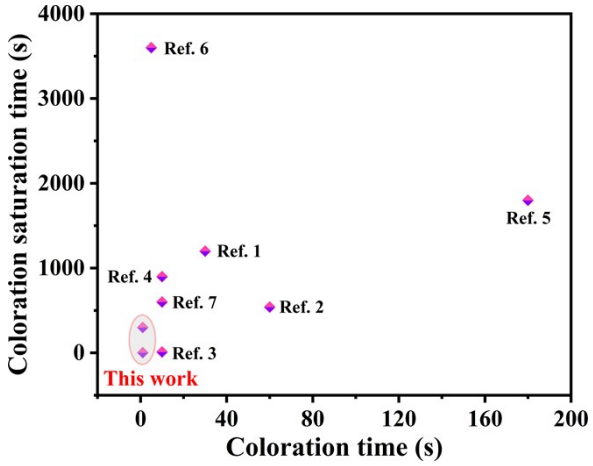

Fig. S3. Summary of photochromic CPs in the literature compared to this work.

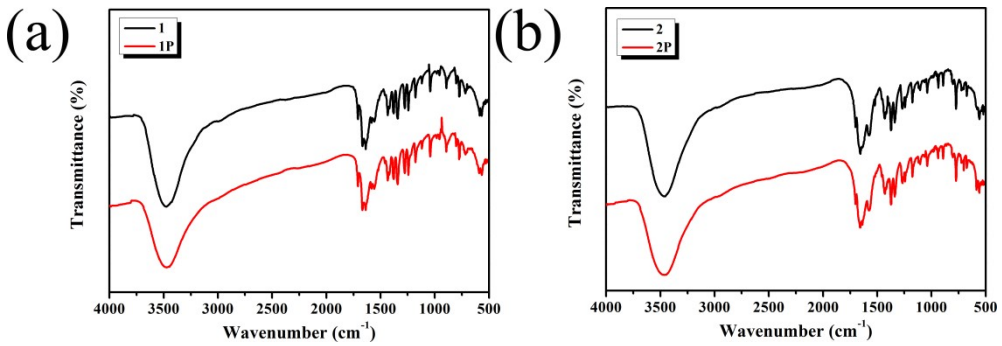

Fig. S4. (a) FT-IR spectra of **1** and **1P**. (b) FT-IR spectra of **2** and **2P**.

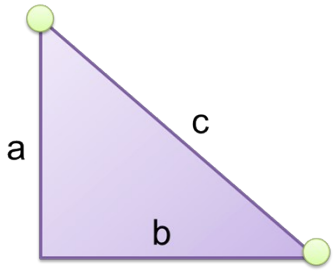

a = Centroid to plane vertical distance
b = Centroid to centroid slippage distance
c = Centroid to centroid distance
Pythagorean theorem: $a^2 + b^2 = c^2$
b = $\sqrt{c^2 - a^2}$

Fig. S5. The calculation principle of DORS

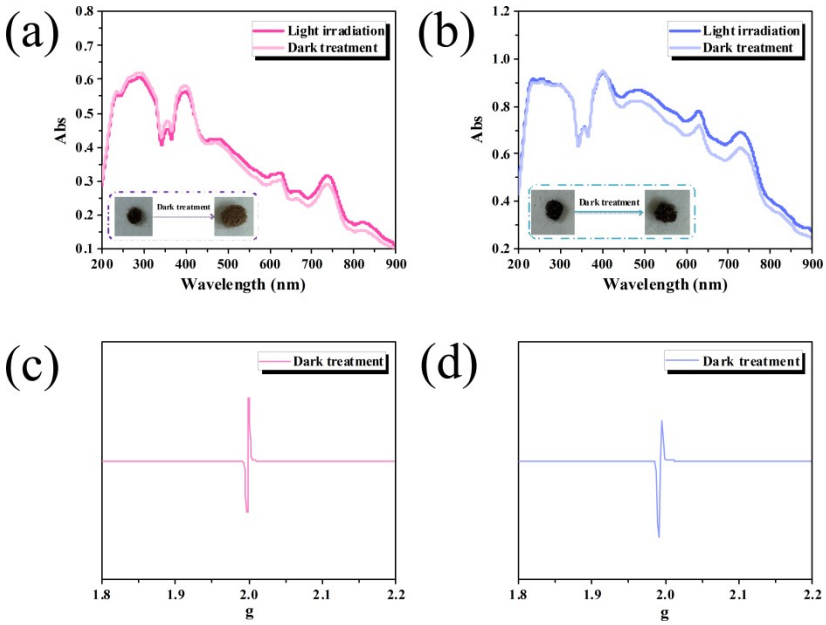

Fig. S6. (a) The UV-vis absorption spectra of **1** after dark treatment (insert: electronic picture of **1** after dark treatment). (b) The UV-vis absorption spectra of **2** after dark treatment (insert: electronic picture of **2** after dark treatment). (c) EPR spectra of **1** after dark treatment. (d) EPR spectra of **2** after dark treatment.

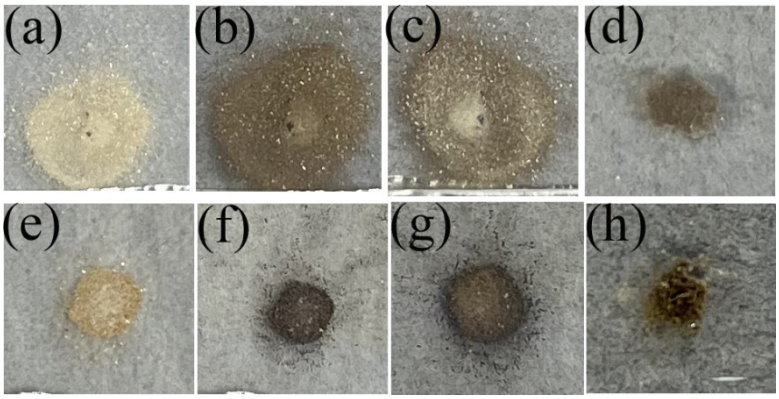

Fig. S7. (a) Primary sample of **1**. (b) Electronic picture of **1** after UV light irradiation. (c) Back side of **1**. (d) Electronic picture of **1** after grind. (e) Primary sample of **2**. (f) Electronic picture of **2** after UV light irradiation. (g) Back side of **2**. (h) Electronic picture of **2** after grind.

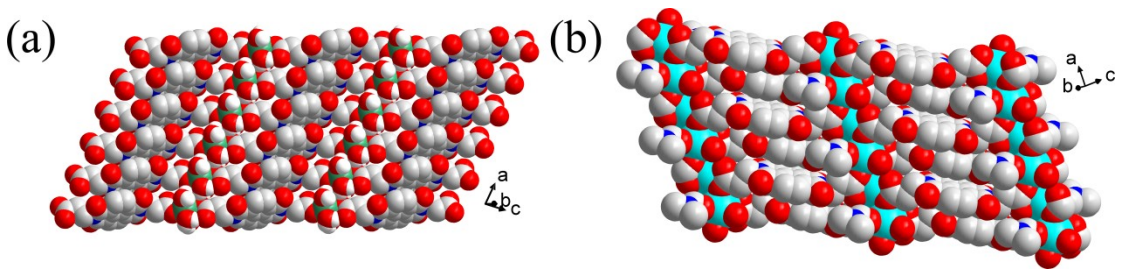

Fig. S8. (a) the space-filling view of **1**. (b) the space-filling view of **2**.

2. Table

Table S1. Crystallographic data and refinement parameters of **1** and **1P**.

Compound	**1**	**1P**
CCDC Code	2394240	2394241
Empirical formula	$C_{20}H_{20}N_2O_{12}Mg$	$C_{20}H_{20}N_2O_{12}Mg$
Formula weight	504.69	504.69
Temperature (K)	293(2)	293(2)
Crystal system	triclinic	triclinic
Space group	*P*-1	*P*-1
a (Å)	5.0535(12)	5.057(3)
b (Å)	6.3853(16)	6.384(3)
c (Å)	16.505(4)	16.511(8)
α (°)	81.549(6)	81.545(12)
β (°)	82.117(6)	82.082(12)
γ (°)	78.223(7)	78.212(8)
V (Å^3)	512.6(2)	512.9(4)
Z	1	1
D_c (g cm^{-3})	1.635	1.634
μ (mm^{-1})	0.163	0.163
F (000)	262.0	262.0

Radiation	MoKα (λ = 0.71073)	MoKα (λ = 0.71073)
ϑ range (°)	6.568 to 54.992	6.568 to 56.728
Reflections collected	7271	8151
Unique reflections	2358	2546
R_{int}	0.0498	0.0450
Data/restraints/parameters	2358/0/162	2546/0/162
Goodness-of-fit on F^2	1.028	1.010
R_1/wR_2, $[I \geq 2\sigma(I)]^{a,b}$	0.0538/0.1049	0.0472/0.1062
R_1/wR_2, (all data)	0.1051/0.1206	0.0852/0.1218
$\Delta\rho_{max}/\Delta\rho_{min}$ (e Å^{-3})	0.24/-0.28	0.29/-0.29

[a] $R_1 = \sum||F_o|-|F_c||/\sum|F_o|$ [b] $wR_2 = [\sum w(F_o^2-F_c^2)^2/\sum w(F_o^2)^2]^{1/2}$

Table S2. Crystallographic data and refinement parameters of **2** and **2P**.

Compound	**2**	**2P**
CCDC Code	2394242	2394243
Empirical formula	$C_{23}H_{21}N_3O_{10}Sr$	$C_{23}H_{21}N_3O_{10}Sr$
Formula weight	587.05	587.05
Temperature (K)	293(2)	293(2)
Crystal system	triclinic	triclinic
Space group	*P*-1	*P*-1
a (Å)	8.0182(18)	8.019(3)
b (Å)	9.2611(18)	9.258(3)
c (Å)	16.060(4)	16.090(6)
α (°)	84.046(6)	84.054(10)
β (°)	85.142(5)	85.034(10)
γ (°)	84.613(4)	84.591(9)
V (Å^3)	1177.5(5)	1179.3(7)
Z	2	2

D_c (g cm^{-3})	1.656	1.653
μ (mm^{-1})	2.354	2.351
F (000)	596.0	596.0
Radiation	MoKα (λ = 0.71073)	MoKα (λ = 0.71073)
ϑ range (°)	4.438 to 56.658	4.44 to 56.694
Reflections collected	18958	17541
Unique reflections	5864	5865
R_{int}	0.0425	0.0421
Data/restraints/parameters	5864/1/339	5865/1/339
Goodness-of-fit on F^2	1.056	1.031
R_1/wR_2, [$I \geq 2\sigma(I)$][a,b]	0.0307/0.0719	0.0343/0.0750
R_1/wR_2, (all data)	0.0384/0.0747	0.0496/0.0797
$\Delta\rho_{max}/\Delta\rho_{min}$ (e Å^{-3})	0.48/-0.48	0.40/-0.46

[a] $R_1 = \sum||F_o|-|F_c||/\sum|F_o|$ [b] $wR_2 = [\sum w(F_o^2-F_c^2)^2/\sum w(F_o^2)^2]^{1/2}$

Table S3. Selected bond lengths (Å) and angles (°) of **1**.

Compound **1**			
Mg1-O2	2.0993 (16)	Mg1-O3^1	2.0925 (17)
Mg1-O2^1	2.0993 (16)	Mg1-O4^1	2.0626 (16)
Mg1-O3	2.0925 (17)	Mg1-O4	2.0627 (16)
O2^1-Mg1-O2	180.0	O4^1-Mg1-O2^1	90.55 (6)
O3^1-Mg1-O2^1	87.52 (7)	O4^1-Mg1-O2	89.45 (7)
O3-Mg1-O2^1	92.48 (7)	O4-Mg1-O3	91.15 (7)
O3^1-Mg1-O2	92.48 (7)	O4^1-Mg1-O3^1	91.15 (7)
O3-Mg1-O2	87.52 (7)	O4-Mg1-O3^1	88.85 (7)
O3^1-Mg1-O3	180.0	O4^1-Mg1-O3	88.85 (7)
O4-Mg1-O2^1	89.45 (7)	O4^1-Mg1-O4	180.0

O4-Mg1-O2	90.55 (6)

symmetry codes: [1]1-x, 2-y, 1-z; [2]-x, 1-y, -z.

Table S4. Selected bond lengths (Å) and angles (°) of **1P**.

Compound **1P**			
Mg1-O2	2.1034 (15)	Mg1-O3[1]	2.0940 (15)
Mg1-O2[1]	2.1035 (15)	Mg1-O4[1]	2.0624 (15)
Mg1-O3	2.0940 (15)	Mg1-O4	2.0624 (15)
O2[1]-Mg1-O2	180.00 (5)	O4[1]-Mg1-O2[1]	90.56 (6)
O3[1]-Mg1-O2[1]	87.52 (7)	O4[1]-Mg1-O2	89.44 (6)
O3-Mg1-O2[1]	92.59 (7)	O4-Mg1-O3	91.15 (7)
O3[1]-Mg1-O2	92.59 (7)	O4[1]-Mg1-O3[1]	91.15 (7)
O3-Mg1-O2	87.41 (7)	O4-Mg1-O3[1]	88.85 (7)
O3[1]-Mg1-O3	180.0	O4[1]-Mg1-O3	88.85 (7)
O4-Mg1-O2[1]	89.44 (6)	O4[1]-Mg1-O4	180.0
O4-Mg1-O2	90.56 (6)		

symmetry codes: [1]1-x, 2-y, 1-z; [2]-x, 1-y, -z.

Table S5. Selected bond lengths (Å) and angles (°) of **2**.

Compound **2**			
Sr1-O1	2.6039 (16)	Sr1-O4[1]	2.8056 (16)
Sr1-O2	2.4846 (19)	Sr1-O9[2]	2.6533 (15)
Sr1-O3[1]	2.6095 (14)	Sr1-O10[3]	2.4958 (14)
Sr1-O3	2.5123 (15)	Sr1-O10[2]	2.6017 (14)
O1-Sr1-O3[1]	161.74 (5)	O3[1]-Sr1-O9[2]	93.04 (5)

O1-Sr1-O4^{1}	150.26 (5)	O3-Sr1-O9^{2}	79.34 (5)
O1-Sr1-O9^{2}	76.61 (6)	O3-Sr1-O10^{2}	128.54 (4)
O2-Sr1-O1	94.86 (7)	O9^{2}-Sr1-O4^{1}	110.71 (5)
O2-Sr1-O3	77.22 (6)	O10^{3}-Sr1-O1	79.54 (5)
O2-Sr1-O3^{1}	88.25 (7)	O10^{2}-Sr1-O1	74.28 (5)
O2-Sr1-O4^{1}	88.52 (7)	O10^{3}-Sr1-O3	153.24 (5)
O2-Sr1-O9^{2}	154.86 (6)	O10^{3}-Sr1-O3^{1}	118.68 (5)
O2-Sr1-O10^{2}	151.19 (6)	O10^{2}-Sr1-O3^{1}	110.51 (5)
O2-Sr1-O10^{3}	78.59 (6)	O10^{3}-Sr1-O4^{1}	72.18 (4)
O3-Sr1-O1	91.25 (5)	O10^{2}-Sr1-O4^{1}	88.69 (4)
O3-Sr1-O3^{1}	71.87 (5)	O10^{3}-Sr1-O9^{2}	121.85 (4)
O3-Sr1-O4^{1}	118.24 (4)	O10^{2}-Sr1-O9^{2}	49.45 (4)
O3^{1}-Sr1-O4^{1}	47.60 (4)	O10^{3}-Sr1-O10^{2}	73.27 (5)

symmetry codes: ^{1}2-x, 1-y, -z; ^{2}-x+1, -y, 1-z; ^{3}x, 1+y, 1-z.

Table S6. Selected bond lengths (Å) and angles (°) of **2P**.

Compound **2P**			
Sr1-O1	2.6029 (19)	Sr1-O4^{1}	2.6542 (17)
Sr1-O2	2.481 (2)	Sr1-O9^{2}	2.8042 (19)
Sr1-O3	2.4989 (16)	Sr1-O10^{3}	2.5151 (17)
Sr1-O3^{1}	2.6027 (16)	Sr1-O10^{2}	2.6103 (17)
O1-Sr1-O4^{1}	76.57 (7)	O3-Sr1-O4^{1}	121.91 (5)
O1-Sr1-O9^{2}	150.21 (6)	O3^{1}-Sr1-O9^{2}	88.61 (5)
O1-Sr1-O10^{2}	161.74 (6)	O3-Sr1-O9^{2}	72.10 (5)
O2-Sr1-O1	95.11 (8)	O3-Sr1-O10^{3}	153.27 (6)
O2-Sr1-O3^{1}	151.28 (6)	O3^{1}-Sr1-O10^{2}	110.39 (6)
O2-Sr1-O3	78.58 (6)	O3-Sr1-O10^{2}	118.65 (5)

O2-Sr1-O4[1]	154.92 (7)	O4[1]-Sr1-O9[2]	110.77 (6)
O2-Sr1-O9[2]	88.31 (7)	O10[3]-Sr1-O1	91.12 (6)
O2-Sr1-O10[3]	77.36 (6)	O10[3]-Sr1-O3[1]	128.42 (5)
O2-Sr1-O10[2]	88.10 (7)	O10[2]-Sr1-O4[1]	93.01 (5)
O3-Sr1-O1	79.58 (6)	O10[3]-Sr1-O4[1]	79.18 (5)
O3[1]-Sr1-O1	74.32 (6)	O10[3]-Sr1-O9[2]	118.42 (5)
O3-Sr1-O3[1]	73.30 (6)	O10[2]-Sr1-O9[2]	47.64 (5)
O3[1]-Sr1-O4[1]	49.49 (5)	O10[3]-Sr1-O10[2]	72.01 (6)

symmetry codes: [1]1-x, 2-y, -z; [2]-x, 1-y, 1-z; [3]x, 1+y, z-1.

Table S7. Hydrogen bonds of **1** (Å and °).

Compound **1**				
D-H···A	d(D-H)	d(H···A)	d(D···A)	<(DHA)
O3-H3A···O1[1]	0.85	1.93	2.760 (3)	163
O3-H3B···O2[2]	0.85	2.24	3.073 (3)	166
O4-H4A···O1	0.85	1.87	2.653 (2)	153
O4-H4B···O2[3]	0.85	2.24	3.047 (2)	159

Symmetry codes: [1]1-x, 1-y, 1-z; [2]-x, 2-y, 1-z; [3]1+x, y, z.

Table S8. Hydrogen bonds of **1P** (Å and °).

Compound **1P**				
D-H···A	d(D-H)	d(H···A)	d(D···A)	<(DHA)
O3-H3A···O1[1]	0.85	1.93	2.756 (2)	164
O3-H3B···O2[2]	0.85	2.25	3.075 (2)	165
O4-H4A···O1	0.85	1.87	2.651 (2)	153
O4-H4B···O2[3]	0.85	2.23	3.043 (2)	160

Symmetry codes: [1]1-x, 1-y, 1-z; [2]-x, 2-y, 1-z; [3]1+x, y, z.

Table S9. Hydrogen bonds of **2** (Å and °).

Compound **2**				
D-H···A	d(D-H)	d(H···A)	d(D···A)	<(DHA)
O1-H1A···O4[1]	0.85	2.02	2.838 (2)	161
O1-H1B···O7[2]	0.85	2.07	2.908 (2)	170
Symmetry codes: [1]1-x, y, z; [2]1-x, 1-y, 1-z.				

Table S10. Hydrogen bonds of **2P** (Å and °).

Compound **2P**				
D-H···A	d(D-H)	d(H···A)	d(D···A)	<(DHA)
O1-H1A···O9[1]	0.85	2.02	2.837 (3)	161
O1-H1B···O6[2]	0.85	2.06	2.907 (3)	171
Symmetry codes: [1]1+x, 1+y, z-1;[2]1-x, 1-y, -z.				

Table S11. Summary of photochromic parameters in the literature compared to this work.

Compound	Pack	Light source	Ring-slippage (Å)	$d_{\pi-\pi}$ (Å)	Ref.
[Zn(NDI-ATZ)(DMF)$_2$]	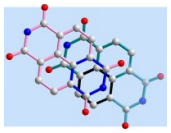	Sunlight	0.854	3.778	8
[Ca(BIPNDI)$_{0.5}$(DMF)$_2$]	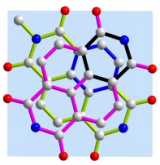	Xe lamp >420 nm	0.877	3.778	9

RC	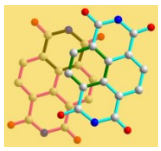	UV	2.010	3.887	10
2	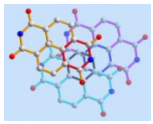	Xe lamp >420 nm	1.172	3.607	This work
1	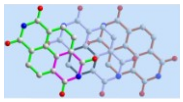	Xe lamp >420 nm	1.483	3.683	This work
MC	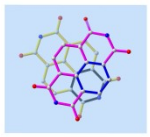	Xe lamp >420 nm	0.759	3.587	11

Table S12. The change of single-crystal parameters before and after UV light irradiation.

Parameters	**1**	**1P**	**2**	**2P**
a (Å)	5.054	5.057	8.018	8.019
b (Å)	6.385	6.384	9.261	9.258
c (Å)	16.506	16.511	16.060	16.090
α (°)	81.549	81.545	84.046	84.054
β (°)	82.117	82.082	85.142	85.034
γ (°)	78.223	78.212	84.613	84.591
V (Å$^{3)}$	512.6	512.9	1177.5	1179.3
π-π interactions (Å)	3.683	3.685	3.607 3.727	3.615 3.730

References

1. C. Fu, G. S. Zhang and H. Y. Wang, et al. Different photochromic properties induced by lone pair–π interactions with varying strengths in two stereocontrolled self-assembly isomeric coordination polymers, CrystEngComm, 2018, **20**, 6821–6827.

2. J. J. Liu, Z. J. Wang and S. B. Xia, et al. Photochromic and photocontrolled luminescence properties of two metalorganic frameworks constructed from a

naphthalene diimide derivative, Dyes Pigm., 2020, **172**, 107856.

3. P. F. Hao, B. H. Gao and G. P. Li, et al. Ultrafast visible-light photochromic properties of naphthalenediimide-based coordination polymers for the visual detection/filtration of blue light, Inorg. Chem. Front., 2022, **9**, 2852–2861.

4. P. F. Hao, H. H. Zhu and Y. Pang, et al. The impact of positional isomerism on electronic and photochromic properties of 1-D zinc-based naphthalene diimide coordination polymers, CrystEngComm, 2020, **22**, 3371–3377.

5. H. H. Zhu, P. F. Hao and Q. Shen, et al. The modulation effect of electron-rich solvents on the supramolecular networks and photochromic properties of naphthalene diimide molecules, CrystEngComm, 2021, **23**, 3356–3363.

6. G. P. Li, H. H. Zhu and P. F. Hao, et al. The modulation effect of carboxylic acid ligands on the electron transfer photochromism of NDI derived coordination polymers, Dalton Trans., 2021, **50**, 15153–15161.

7. P. F. Hao, H. H. Zhu and Y. Pang, et al. Positional isomerism controlled electronic and photochromic properties of naphthalene diimide-based chlorozincate hybrids, Cryst. Growth Des., 2020, **20**, 345−351.

8. Y. X. Xie, W. N. Zhao and G. C. Li, et al. A naphthalenediimide-based metal−organic framework and thin film exhibiting photochromic and electrochromic properties, Inorg. Chem., 2016, **55**, 549−551.

9. M. H. You, M. H. Li and H. H. Li, et al. The impact of metal cations on the photochemical properties of hybrid heterostructures with infinite alkaline-earth metal oxide clusters, Dalton Trans., 2019, **48**, 17381−17387.

10. S. M. Zhang, P. F. Hao and Y. F. Zhang, et al. The simultaneous modulation effect of *N*-substituents on the photochromic and electrochromic properties of naphthalenediimide-based coordination polymers, Inorg. Chem. Front., 2024, **11**, 1226–1237.

11. L. Qin, W. N. Zhao and G. J. Yu, et al. A zinc-organic coordination polymer of glycine-functionalized naphthalenediimide ligand, Inorg. Chem. Commun., 2013, 34, 47–50.